JACS
JOURNAL OF THE AMERICAN CHEMICAL SOCIETY
Article
pubs.acs.org/JACS

The Quest for Converting Biorenewable Bifunctional α-Methylene-γ-butyrolactone into Degradable and Recyclable Polyester: Controlling Vinyl-Addition/Ring-Opening/Cross-Linking Pathways

Xiaoyan Tang,[†] Miao Hong,[†] Laura Falivene,[‡] Lucia Caporaso,[§] Luigi Cavallo,*[,‡,§] and Eugene Y.-X. Chen*[,†]

[†]Department of Chemistry, Colorado State University, Fort Collins, Colorado 80523-1872, United States

[‡]Physical Sciences and Engineering Division, Kaust Catalysis Center, King Abdullah University of Science and Technology (KAUST), Thuwal 23955-6900, Saudi Arabia

[§]Dipartimento di Chimica e Biologia, Università di Salerno, Via Papa Paolo Giovanni II, I-84084, Fisciano, Italy

Supporting Information

ABSTRACT: α-Methylene-γ-butyrolactone (MBL), a naturally occurring and biomass-sourced bifunctional monomer, contains both a highly reactive exocyclic C═C bond and a highly stable five-membered γ-butyrolactone ring. Thus, all previous work led to exclusive vinyl-addition polymerization (VAP) product $P(MBL)_{VAP}$. Now, this work reverses this conventional chemoselectivity to enable the first ring-opening polymerization (ROP) of MBL, thereby producing exclusively unsaturated polyester $P(MBL)_{ROP}$ with M_n up to 21.0 kg/mol. This elusive goal was achieved through uncovering the thermodynamic, catalytic, and processing conditions. A third reaction pathway has also been discovered, which is a crossover propagation between VAP and ROP processes, thus affording cross-linked polymer $P(MBL)_{CLP}$. The formation of the three types of polymers, $P(MBL)_{VAP}$, $P(MBL)_{CLP}$, and $P(MBL)_{ROP}$, can be readily controlled by adjusting the catalyst (La)/initiator (ROH) ratio, which is determined by the unique chemoselectivity of the La−X (X = OR, NR_2, R) group. The resulting $P(MBL)_{ROP}$ is degradable and can be readily postfunctionalized into cross-linked or thiolated materials but, more remarkably, can also be fully recycled back to its monomer thermochemically. Computational studies provided the theoretical basis for, and a mechanistic understanding of, the three different polymerization processes and the origin of the chemoselectivity.

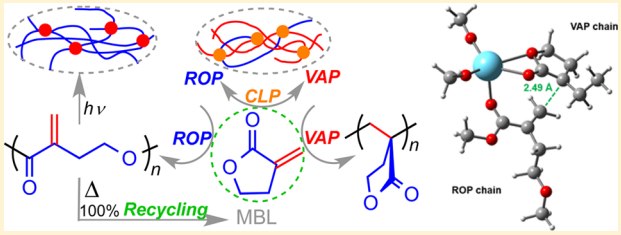

INTRODUCTION

Efforts toward the development of sustainable polymers have been chiefly directed at renewable polymers based on naturally occurring or biomass-derived renewable feedstocks.[1] However, an emerging frontier in sustainable polymers is the design and synthesis of recyclable polymers that can be completely depolymerized to their monomers either thermally,[2] mechanically,[3] or chemically,[4] the recovered building blocks of which can then be reused to produce virgin quality polymers. The task of developing completely recyclable polymers is a challenge; using the biorenewable and biodegradable poly(L-lactide) as an example, thermal degradation of this polymer as a possible feedstock-recycling pathway produced many kinds of degradation products including lactide diastereomers, cyclic oligomers and their diastereomers, as well as small molecules such as CO_2, CO, CH_3CHO, and CH_2═CHCOOH.[5] Chemical recyclability is essential for developing truly sustainable polymers that are not only biorenewable and degradable, but also recyclable and accessible via a greener or sustainable process,[6] thereby achieving the possible circular economy. However, the classes of fully recyclable polymers are very limited, and the polymers that can be easily depolymerized often suffer from their undesired thermal and mechanical properties for poor materials performance. Thus, more intensive research is needed to identify new renewable polymer systems that can strike a balance between their recyclability and thermal stability or mechanical strength.

Found naturally in tulips or produced chemically from biomass feedstocks, tulipalin A, or α-methylene-γ-butyrolactone (MBL), is the simplest member of the sesquiterpene lactone family[7] and the most studied monomer of the biobased tulipalin family for biorenewable polymers.[8] MBL, along with its methyl-substituted derivatives, γ-methyl-α-methylene-γ-butyrolactone ($_\gamma$MMBL)[9] and β-methyl-α-methylene-γ-butyrolactone ($_\beta$MMBL),[10] derived from biomass-sourced levulinic and itaconic acids, respectively, exhibits higher reactivity and forms polymers with superior materials properties, relative to its linear analog methyl methacrylate (MMA), thereby receiving a renaissance of interest in the prospects of offering a renewable alternative to the petroleum-based MMA for the production of specialty chemicals and acrylic bioplastics.[8] For example, the

Received: August 1, 2016
Published: October 4, 2016

DOI: 10.1021/jacs.6b07974
J. Am. Chem. Soc. 2016, 138, 14326−14337

atactic PMMA has a typical glass-transition temperature (T_g) of 105 °C and is soluble in common organic solvents, whereas the polymers derived from MBL, $_{\gamma}$MMBL, and $_{\beta}$MMBL exhibit much higher T_g values of 195 °C, 227 °C, and 288 °C, respectively, and are more solvent resistant. In this context, various types of polymerization processes have been employed to polymerize such renewable methylene lactones including radical,[11] anionic,[12] zwitterionic,[13] group-transfer,[14] organocatalytic,[15] and coordination[16] polymerization methods. Regardless of the method, however, the processes reported to date follow exclusively the vinyl-addition polymerization (VAP) pathway to produce the corresponding VAP polymer, $P(MBL)_{VAP}$, through conjugate addition across the highly reactive exocyclic C=C double bond, without ring-opening of the highly stable five-membered γ-butyrolactone (γ-BL) ring.

An intriguing fundamental question is whether one could reverse this conventional chemoselectivity by turning on the ring-opening polymerization (ROP) of MBL while shutting down the VAP process, which would enable the synthesis of biorenewable and degradable unsaturated polyester, the corresponding ROP polymer, $P(MBL)_{ROP}$ (Scheme 1). Such

Scheme 1. VAP of MBL of All Previous Work versus the ROP and CLP of MBL of the Current Work That Led to Either Recyclable and Postfunctionalizable Unsaturated Polyester $P(MBL)_{ROP}$ or Cross-Linked Polymer $P(MBL)_{CLP}$

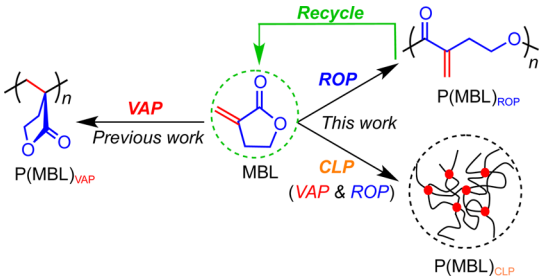

unsaturated polyester will provide a needed functional (reactive double bond) handle for postfunctionalization to tailor-made polyester materials,[17] which currently lacks in the aliphatic polyesters prepared by the ROP of typical lactones and lactides.[18] Chemoselective ROP of an *exo*-methylene macrolactone, 2-methylene-4-oxa-12-dodecanolide, was achieved with lipase catalysis.[19] However, achievement of this objective requires meeting two challenges: the high reactivity of the exocyclic C=C double bond (vide supra) and the high stability of the γ-BL ring (vide infra) present in MBL, both of which point to the exclusive VAP pathway observed to date. In fact, the nonstrained γ-BL was commonly referred as "non-polymerizable" in textbooks[20] and literature.[21] The non-polymerizability observed in the ROP of γ-BL under ambient pressure[22] can be explained by its unfavorable thermodynamics as there was a large negative entropic change (ΔS_p°) and a small positive change of enthalpy (ΔH_p°) (which was later showed to be small negative, therefore exhibiting a low ceiling temperature of polymerization[2]) that gave rise to a positive Gibbs free energy of polymerization.[23] Recently, we discovered thermodynamic, catalytic, and processing conditions that enabled the first successful chemical ROP of γ-BL into high molecular weight (MW) poly(γ-BL), PγBL, with controlled linear or cyclic topologies and complete thermal recyclability by simply heating the bulking material at 220 °C (for the linear polymer) or 300 °C (for the cyclic polymer) under readily accessible conditions (i.e., 1 atm, −40 °C, THF).[2] In that process, metal (La, Y)-catalyzed coordination ROP was found to be the most effective method to achieve high MW PγBL and high monomer conversion. Most recently, we also reported the organocatalytic ROP of γ-BL to high MW PγBL, which established PγBL as a truly sustainable material.[6]

However, enabling the ROP of the bifunctional MBL, known to favor VAP and resist ROP, is even more challenging due to the additional obstacle to control the chemoselectivity. A known strategy to ring-open polymerize MBL is to copolymerize it with a lactone having high ring strain energy such as ε-caprolactone (ε-CL).[24,25] This ring-opening copolymerization (ROC) approach has indeed produced copolyester $P(MBL)_{ROP}$-*co*-PCL. Interestingly, we found that, while performing the ROC by $Bi(OTf)_3$ at 130 °C[24] led to a mixture of ROP copolymer $P(MBL)_{ROP}$-*co*-PCL and VAP homopolymer $P(MBL)_{VAP}$,[25] carrying out the ROC by lanthanide (Ln)-based coordination polymerization catalysts at subzero temperatures greatly favored incorporation of the ring-opened MBL into the copolyester, thus achieving $P(MBL)_{ROP}$-*co*-PCL with the MBL incorporation up to 40 mol % and without formation of $P(MBL)_{VAP}$.[25] On the basis of these earlier results, we hypothesized that uncovering the thermodynamic, catalytic, and processing conditions could eventually lead to a homopolymerization system that renders the ROP of MBL to produce exclusively unsaturated polyester $P(MBL)_{ROP}$, the central objective of this work, which has been achieved for the first time through this study. In addition, by judiciously choosing the catalyst/initiator ratio and reaction conditions, VAP and ROP can both occur and cross-propagate in the polymerization, thus leading to cross-linked polymer $P(MBL)_{CLP}$. Furthermore, as MBL contains the γ-BL ring, we reasoned that the resulting ROP polymer $P(MBL)_{ROP}$ should be readily recyclable just like PγBL. Indeed, $P(MBL)_{ROP}$ can not only be readily postfunctionalized via photocuring and the thiol−ene click reaction, but also it can also be fully recycled back to the monomer MBL after heating its solution at ≥100 °C for 1 h in the presence of a simple catalyst (Scheme 1).

RESULTS AND DISCUSSION

Chemoselectivity of MBL Polymerization: VAP versus ROP versus CLP. At the outset, lanthanum complex $La[N(SiMe_3)_2]_3$ (**1**, Chart 1), which has been shown to be

Chart 1. Three Metal-Based Catalysts, Homoleptic La Complex 1 and Heteroleptic Discrete Single-Site Y Complexes 2 and 3, Employed in This Study

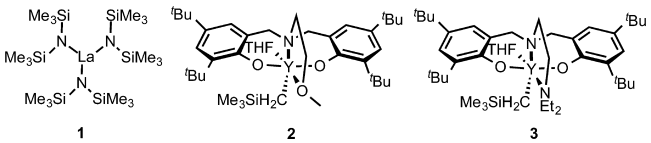

an effective catalyst for the ROP of γ-BL,[2] was used for initial screening of MBL polymerization. As anticipated, at room temperature it mediated rapid VAP, with or without addition of initiator BnOH, thus leading to exclusive formation of $P(MBL)_{VAP}$ (runs 1−4, Table S1, Figure 1iii). To realize the possible ROP of MBL, subsequent polymerizations were conducted at low temperatures, ranging from −40 °C to −78 °C in THF, with different alcohol initiators, and in varied [MBL]/[La]/[ROH] ratios, the results of which were

DOI: 10.1021/jacs.6b07974
J. Am. Chem. Soc. 2016, 138, 14326−14337

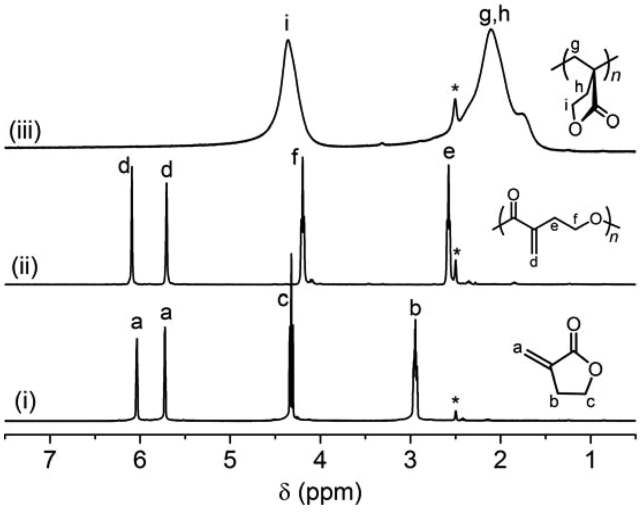

Figure 1. Overlay of ^{1}H NMR spectra (DMSO-d_6, residual peak marked as ∗) of (i) MBL, (ii) P(MBL)$_{ROP}$, and (iii) P(MBL)$_{VAP}$.

summarized in Table 1. At −60 °C with a 1.0 mol % loading of **1** and [MBL] = 5.0 M (the maximum concentration achievable in THF at this temperature), the polymerization still gave the VAP product P(MBL)$_{VAP}$ (run 1, Table 1). As alcohols react readily with lanthanide amides via in situ alcoholysis to generate Ln alkoxides, which usually exhibit superior performances and mediate more controllable ROP of cyclic esters than the corresponding amido analogues,[2,26−28] we introduced alcohol into the catalyst system. Interestingly, with La/BnOH = 1:1, only insoluble, cross-linked polymer product P(MBL)$_{CLP}$ was obtained (run 2). By changing the La/BnOH ratio to 1:2, a mixture of CLP, VAP, and ROP polymer products was produced (run 3). Excitingly, the exclusive formation of ROP product P(MBL)$_{ROP}$ was achieved with La/BnOH = 1:3 (runs 4−6). Under such conditions, the P(MBL)$_{ROP}$ produced had a low MW of M_n = 5.5 kg/mol and a narrow MW distribution of $Đ$ = 1.16 (run 6). Changing the MBL/La/BnOH ratio from 100:1:3 to 200:1:3 enhanced the MW of P(MBL)$_{ROP}$ to M_n = 10.4 kg/mol (run 7). Overall, the above results indicate that the La−NR$_2$ group exhibits a preference for VAP, while the La−OBn group favors ROP. A control run with the isolated [La(OBn)$_3$]$_n$ led to formation of the same ROP product

Table 1. Results of MBL Polymerization in THF by Ln/ROH Catalyst/Initiator Systems[a]

run no.	catalyst	initiator (I)	[MBL]/[cat]/[I]	MBL (M)	temperature (°C)	time (h)	yield[b] mg (%)	M_n[c] (kg/mol)	$Đ$[c] (M_w/M_n)	chemoselectivity (polymer type)
1	**1**		100:1	5.0	−60	3	110 (22)	54.2	2.85	VAP
2	**1**	BnOH	100:1:1	5.0	−60	24	74 (15)	n.d.	n.d.	CLP
3	**1**	BnOH	100:1:2	5.0	−60	24	100 (20)	n.d.	n.d.	VAP+ROP+CLP
4	**1**	BnOH	100:1:3	5.0	−60	12	51 (10)	5.1	1.16	ROP
5	**1**	BnOH	100:1:3	5.0	−60	17	145 (30)	5.0	1.26	ROP
6	**1**	BnOH	100:1:3	5.0	−60	24	158 (32)	5.5	1.16	ROP
7	**1**	BnOH	200:1:3	5.0	−60	24	156 (32)	10.4	1.28	ROP
8		[La(OBn)$_3$]$_n$	100:1	5.0	−60	24	108 (22)	5.2	1.21	ROP
9	**1**	BnOH	100:1:3	2.0	−60	24	trace	n.d.	n.d.	CLP
10	**1**	BnOH	100:1:3	2.0	−78	24	9 (1.8)	n.d.	n.d.	CLP
11	**1**	BnOH	100:1:3	8.0	−40	24	95 (19)	5.0	1.28	ROP
12	**1**	BnOH	100:1:3	5.0	−40	24	14 (2.9)	n.d.	n.d.	CLP
13	**1**	BnOH	100:1:2	8.0	−40	16	409 (84)	n.d.	n.d.	CLP
14	**1**	BnOH	100:1:2	5.0	−40	16	320 (65)	n.d.	n.d.	VAP+CLP
15	**1**	Ph$_2$CHCH$_2$OH	100:1:1	5.0	−60	24	108 (22)	n.d.	n.d.	VAP+ROP+CLP
16	**1**	Ph$_2$CHCH$_2$OH	100:1:2	5.0	−60	12	184 (38)	n.d.	n.d.	VAP+ROP+CLP
17	**1**	Ph$_2$CHCH$_2$OH	100:1:3	5.0	−60	12	136 (28)	5.8	1.23	ROP
18[d]	**1**	Ph$_2$CHCH$_2$OH	100:1:3	5.0	−60	24	209 (43)	5.3	1.24	ROP
19	**1**	Ph$_2$CHCH$_2$OH	200:1:3	5.0	−60	24	205 (42)	6.7	1.17	ROP
20	**1**	Ph$_2$CHCH$_2$OH	100:1:3	8.0	−40	24	59 (12)	5.3	1.21	ROP
21	**1**	^{i}PrOH	100:1:1	5.0	−60	24	152 (31)	n.d.	n.d.	VAP+ROP+CLP
22	**1**	^{i}PrOH	100:1:2	5.0	−60	16	161 (33)	n.d.	n.d.	VAP+ROP+CLP
23	**1**	^{i}PrOH	100:1:3	5.0	−60	12	66 (14)	4.6	1.45	ROP
24	**1**	^{i}PrOH	100:1:3	5.0	−60	24	172 (35)	4.7	1.15	ROP
25	**1**	^{i}PrOH	200:1:3	5.0	−60	24	155 (32)	5.6	1.19	ROP
26	**2**		100:1	5.0	−60	4	140 (29)	16.9	1.53	ROP
27	**2**		100:1	5.0	−60	6	170 (35)	14.3	1.79	ROP
28	**2**		100:1	5.0	−60	12	251 (51)	18.3	1.75	ROP
29	**2**		200:1	5.0	−60	5	138 (28)	18.3	1.76	ROP
30	**2**		200:1	5.0	−60	12	198 (40)	21.0	1.75	ROP
31[e]	**2**		100:1	5.0	−60	12	**2700 (55)**	**21.0**	**1.42**	ROP
32	**3**		100:1	5.0	−60	24	24 (4.9)	10.6	1.19	ROP

[a]Conditions: MBL = 0.49 g (5.0 mmol); the catalyst and initiator amount varied according to [MBL]/[cat]/[I] molar ratio; n.d. = not determined (M_n and $Đ$ not determined due to cross-linking). [b]Isolated polymer yield. [c]M_n and $Đ$ determined by GPC at 40 °C in DMF relative to PMMA standards. [d]The monomer conversion was 52%. No polymer precipitation occurred with 1 h, but occurred after a few hours. The reaction mixture was solidified within 12 h. [e]MBL = 4.9 g (50 mmol), [MBL] = 5.0 M in THF (5.6 mL).

DOI: 10.1021/jacs.6b07974
J. Am. Chem. Soc. 2016, 138, 14326−14337

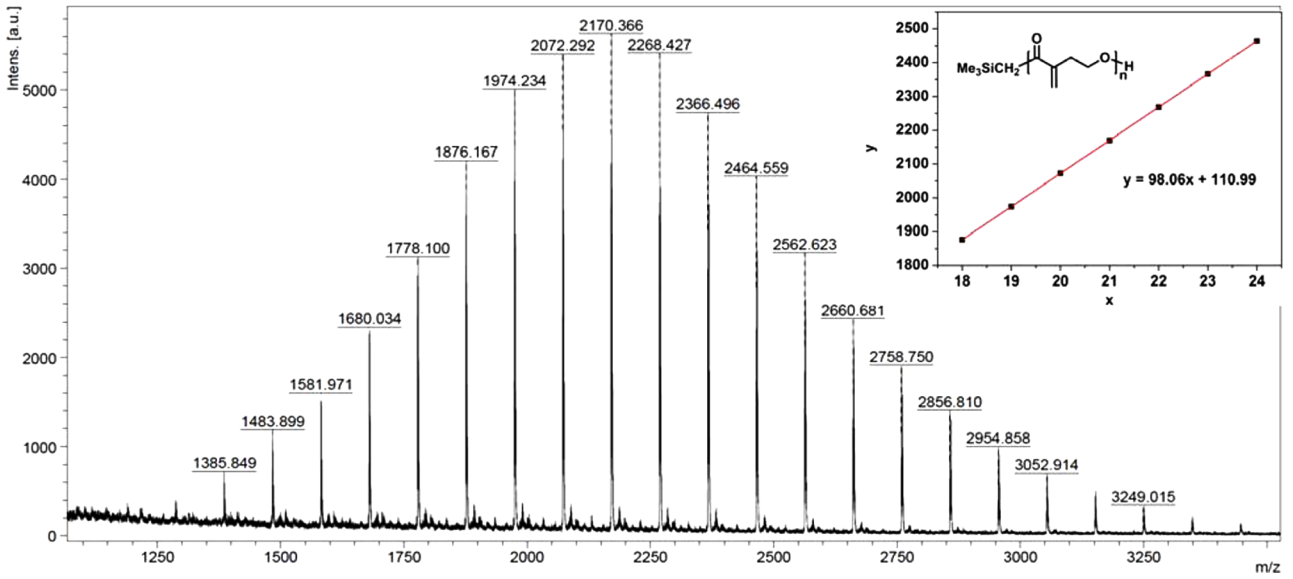

Figure 2. MALDI-TOF spectrum of $P(MBL)_{ROP}$ produced with yttrium alkyl complex **2**. Inset: plot of m/z values (y) versus the number of MBL repeat units (x).

$P(MBL)_{ROP}$ (run 8), thus supporting the above hypothesis. The theoretical basis for the observed chemoselectivity of the MBL polymerization with respect to the type of initiators (i.e., La−NR_2 vs La−OR) will be discussed in the Computational Study section.

In addition to the above-discussed catalyst (La)/initiator (ROH) ratio, four other factors, including concentration, temperature, initiator, and catalyst, also critically affect the chemoselectivity of the MBL polymerization thus the resulting polymer type. First, relative to the current standard conditions ([MBL]/[La]/[BnOH] = 100:1:3, [MBL] = 5.0 M in THF, −60 °C) that produced $P(MBL)_{ROP}$, decreasing [MBL] from 5.0 to 2.0 M while keeping other conditions the same resulted in formation of only a small amount of cross-linked polymer $P(MBL)_{CLP}$ (run 9); this holds true even when the polymerization was carried out at −78 °C (run 10). Second, increasing the temperature to −40 °C gave only cross-linked polymer $P(MBL)_{CLP}$ (runs 12−14), unless [MBL] was also increased to 8.0 M under which conditions $P(MBL)_{ROP}$ can still be produced (run 11). Third, the chemoselectivity observed for the other two common alcohol initiators, Ph_2CHCH_2OH and ^{i}PrOH (runs 15−25), was the same as that seen for BnOH, that is, under the current standard conditions, only when {[MBL]/[La]/[ROH]} = 100:1:3, pure $P(MBL)_{ROP}$ was produced. Among the three ROH initiators, the sterically bulkier alcohol Ph_2CHCH_2OH achieved the highest monomer conversion (52%) and thus gave the best isolated ROP product yield of 43% (run 18), which is attributable to its steric bulk that can effectively suppress the aggregation of the resulting $[La(OCH_2CHPh_2)_3]_n$ active species to form higher clusters.[2] Fourth, discrete, single-site yttrium alkyl complex **2** (Chart 1, Figure S1),[26] supported by a tetradentate, dianionic amino-bisphenolate ligand bearing a pendant ether group and previously revealed as a superior catalyst for the ROP of γ-BL,[2] also gave the best performance in the ROP of MBL (runs 26-31), producing $P(MBL)_{ROP}$ with M_n up to 21.0 kg/mol (run 30, Figure 1ii). A multigram scale of the ROP of MBL (4.90 g) by **2** produced exclusively $P(MBL)_{ROP}$ with M_n = 21.0 kg/mol and $Đ$ = 1.42 in 55% isolated yield (run 31). Intriguingly, a minor yet subtle change in the Y catalyst structure from the pendant ether group in **2** to the pendant amino group in **3** (Figure S2)[27] resulted in a drastic drop in the ROP product yield to only 4.9% (run 32).

Thermodynamic and Mechanistic Considerations. To shed light on why the ROP of MBL requires a low temperature and a high monomer concentration, typically at −60 °C and 5.0 M, we measured the thermodynamics of the polymerization under conditions of MBL/**1**/Ph_2CHCH_2OH = 100:1:3 and $[MBL]_0$ = 5.0 M in CD_2Cl_2, through variable temperature NMR studies at low temperatures. Worth noting here is that, in contrast to the polymerizations carried out in THF (Table 1), which were performed under heterogeneous, nonequilibrium conditions where the resulting polymer precipitates out of the reaction medium so that the conversion can far exceed the thermodynamic limit, the current experiments of measuring the thermodynamic parameters were performed in CD_2Cl_2 (the resulting ring-opening polymer is soluble) to ensure a homogeneous, equilibrium condition for this measurement. First, the equilibrium monomer concentration, $[MBL]_{eq}$, was obtained by plotting $[MBL]_t$ as a function time until the concentration reached a constant (Table S2, Figure S6a). Next, a Van't Hoff plot of $\ln[MBL]_{eq}$ versus $1/T$ gave a straight line (Figure S6b), from which thermodynamic parameters were calculated to be ΔH_p = −5.9 kJ mol^{-1} and $\Delta S°_p$ = −40.1 J mol^{-1} K^{-1}, based on the equation $\ln[MBL]_{eq} = \Delta H_p/RT - \Delta S°_p/R$ and in reference to a standard state concentration of monomer of 1 M.[23b] Third, the ceiling temperature (T_c) was calculated to be 221 K (−52 °C) at $[MBL]_0$ = 5.0 M, or 147 K (−126 °C) at $[MBL]_0$ = 1.0 M, based on the equation $T_c = \Delta H_p/(\Delta S°_p + R \ln[MBL]_0)$.[23b] Overall, these values are consistent with the reaction conditions observed experimentally that enabled the ROP of MBL.

To gain insight into the mechanism of the ROP, we determined chain initiation and termination end groups of $P(MBL)_{ROP}$ produced by **1**/ROH (1:3 ratio) with matrix-assisted laser desorption/ionization time-of-flight mass spectroscopy (MALDI-TOF MS) and ^{1}H NMR. As can be seen from Figures S3−S5, the MALDI-TOF MS spectra of the $P(MBL)_{ROP}$ samples prepared with BnOH, Ph_2CHCH_2OH, and ^{i}PrOH showed the same spacing between the two

DOI: 10.1021/jacs.6b07974
J. Am. Chem. Soc. 2016, 138, 14326−14337

neighboring molecular ion peaks being that of the exact molar mass of the repeat unit, MBL (m/z = 98.04), as shown by the slopes of the linear plots of m/z values (y) versus the number of MBL repeat units (x). The intercepts of the plots, 131, 221, and 83, indicated that each $-[(MBL)_{ROP}]_n-$ chain carries RO/H as chain ends [M_{end} = 108 (BnO/H) + 23 (Na^+) g/mol; M_{end} = 198 (Ph_2CHCH_2O/H) + 23 (Na^+) g/mol; M_{end} = 60 (^{i}PrO/H) + 23 (Na^+) g/mol], denoted as RO$-[(MBL)_{ROP}]_n-$H. Likewise, the same analysis of a low MW P(MBL)$_{ROP}$ sample by yttrium alkyl **2** with MALDI-TOF MS (Figure 2) revealed the predicted end groups of Me_3SiCH_2/H: M_{end} (intercept) = 88 (Me_3SiCH_2/H) + 23 (Na^+) = 111 g/mol for the chain structure of $Me_3SiCH_2-[(MBL)_{ROP}]_n-$H. The corresponding ^{1}H NMR spectra of RO$-[(MBL)_{ROP}]_n-$H are depicted in Figure 3, showing, besides the major signals at δ 6.09, 5.71, 4.20, and 2.58 ppm for the main chain protons $-[C(=O)C(=CH_2^{(6.09,\ 5.71)})CH_2^{(2.58)}CH_2^{(4.20)}O]_n-$, minor signals attributed to the chain ends (RO/H). Overall, these results are consistent with the coordination–insertion mechanism for chain initiation and propagation steps (Scheme 2), analogous to that proposed for the ROP of typical cyclic esters[18] and γ-BL.[2]

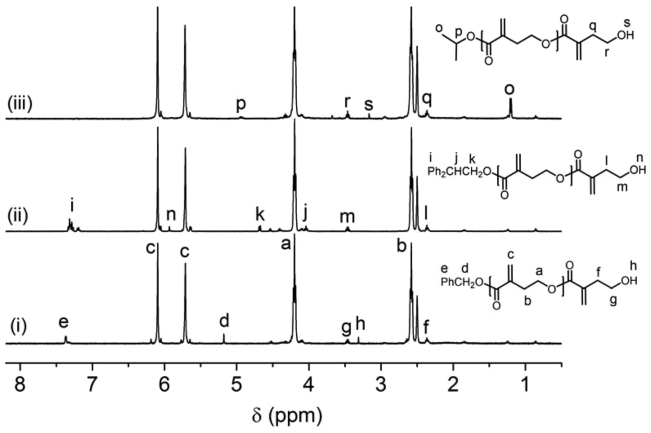

Figure 3. ^{1}H NMR spectra (DMSO-d_6) of RO$-[(MBL)_{ROP}]_n-$H by **1**/ROH (1:3): (i) R = $PhCH_2$, (ii) R = Ph_2CHCH_2, (iii) R = ^{i}Pr.

Scheme 2. Proposed Mechanism for the ROP of MBL by 1 in the Presence of 3 Equiv. ROH (R = Bn, Ph_2CHCH_2, ^{i}Pr)

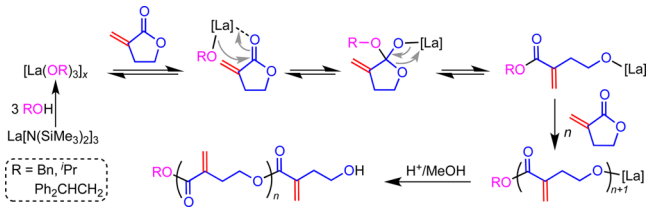

Another intriguing aspect of the MBL polymerization is that the polymerization by **1**/BnOH in a 1:1 ratio at −60 °C produced insoluble cross-linked polymer product P(MBL)$_{CLP}$ (vide supra). This network polymer was shown to contain mainly the P(MBL)$_{VAP}$ chains, as evidenced by their nearly identical FT-IR spectra (Figure S7) and thermal gravimetric analysis (TGA) profiles (Figure S8) between the cross-linked P(MBL)$_{CLP}$ and the linear P(MBL)$_{VAP}$. On the other hand, their differential scanning calorimetry (DSC) curves (Figure S9) are noticeably different, with a T_g of 180.4 and 192.9 °C for P(MBL)$_{CLP}$ and P(MBL)$_{VAP}$, respectively, which is consistent with some more flexible ring-opened ester segments being incorporated into P(MBL)$_{CLP}$. On the basis of the above results and the observations that the La−OR group prefers ROP and the La−NR_2 group prefers VAP, the putative mechanism proposed for the cross-linking process is outlined in Scheme 3. First, bi-initiation (**A**) involves the ring-opening (I) and vinyl-addition (II) pathways via nucleophilic attack of the coordinated (activated) MBL by the −OR and −NR_2 groups to generate (MBL)$_{ROP}$-[La] and (MBL)$_{VAP}$-[La], respectively. Second, homopropagation (**B**) in the VAP pathway leads to the active growing polymer chain P(MBL)$_{VAP}$-[La] containing the active ester enolate chain end. Likewise, species (MBL)$_{ROP}$-[La] can also proceed with homopropagation to afford P(MBL)$_{ROP}$-[La] containing the active alkoxy chain end. Third, cross-propagation (**C**) involves intramolecular Michael addition of P(MBL)$_{VAP}$-[La] to (MBL)$_{ROP}$-[La] or P-(MBL)$_{ROP}$-[La] via eight-membered-ring transition state III, generally accepted for the metal-mediated coordination–addition polymerization of conjugated polar vinyl monomers,[29] producing intermediate IV that contains both VAP and ROP chains as well as both enolate and alkoxy active chain ends for subsequent VAP and ROP processes to furnish cross-linked polymer P(MBL)$_{CLP}$ (Scheme 3).

The key step of this proposed cross-linking process is the cross-propagation step involving transition state III (Scheme 3) for the conjugate-addition of the active center (the enolate) on the vinyl-addition chain, P(MBL)$_{VAP}$-[La], to the vinylidene group on the ROP chain, (MBL)$_{ROP}$-[La] or P(MBL)$_{ROP}$-[La]. The calculated free energy barrier for this step (Chart 2) amounts to only 8.2 kcal/mol, in agreement with the experimental evidence that cross-linked chains were formed when both NR_2 and OR groups reside on the metal, that is, when both the VAP and the ROP pathways can occur and crossover.

Thermal Mechanical Properties and Post-functionalization of P(MBL)$_{ROP}$. Thermal and mechanical properties of P(MBL)$_{ROP}$ produced by the different catalyst/initiator systems were investigated by TGA, DSC, and dynamic mechanical analysis (DMA). TGA and relative derivative thermogravimetry (DTG) curves (Figure S10) of low MW P(MBL)$_{ROP}$ samples (M_n = 4.7–5.8 kg/mol) prepared by **1**/ROH (1:3 ratio) displayed three degradation steps, attributable to extrusion of MBL at the initial step of $T \leq 250$ °C, followed by cross-linking of the pendant double bonds (vide infra) and final decomposition. On the other hand, the higher MW P(MBL)$_{ROP}$ prepared by **2** (M_n = 18.3 kg/mol) showed only the last two degradation steps, also with a higher initial degradation temperature (T_d, defined by the temperature of 5% weight loss) of 293 °C. The T_g measured by DSC (Figure S11) was in the range of −40.2 to −34.9 °C, which increases as an increase in the polymer MW.

To investigate the possible cross-linking while heating, the DSC of P(MBL)$_{ROP}$ prepared by **2** was scanned to a much higher temperature of 400 °C. It is clear from the first heating scan that P(MBL)$_{ROP}$ began to cross-link at ∼250 °C and then decompose at ∼340 °C (Figure S12), after which no subsequent thermal transitions were observed on the first cooling and second heating scan cycles. These results further confirmed that P(MBL)$_{ROP}$ undergoes thermal cross-linking before decomposition. The casted thin film of P(MBL)$_{ROP}$ (M_n = 21.0 kg/mol, $Đ$ = 1.42) was analyzed by DMA (Figure 4), which gave a storage modulus (E') of 3.55 GPa and a loss

DOI: 10.1021/jacs.6b07974
J. Am. Chem. Soc. 2016, 138, 14326–14337

Scheme 3. Proposed Mechanism for the Formation of Cross-Linked Polymer $P(MBL)_{CLP}$ by $La[N(SiMe_3)_2]_3$/BnOH with a Molar Ratio of 1:1 at −60 °C

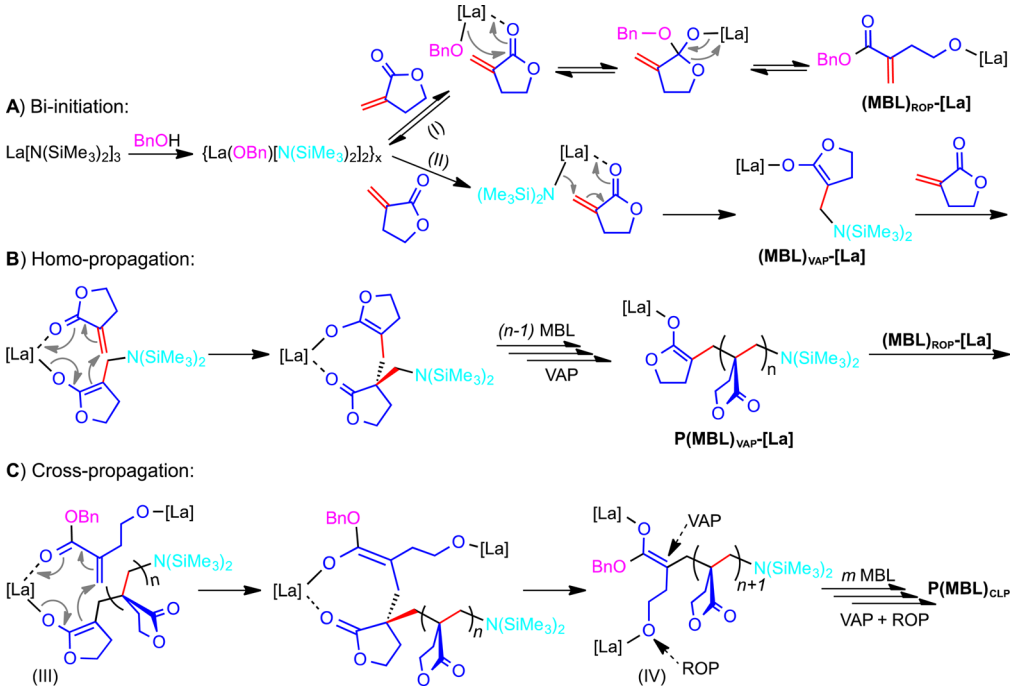

Chart 2. Calculated Transition State for the Cross-Propagation from the VAP Chain End (La Ester Enolate) to the ROP Chain End (La Alkoxide and Vinylidene Group) via Conjugate Addition

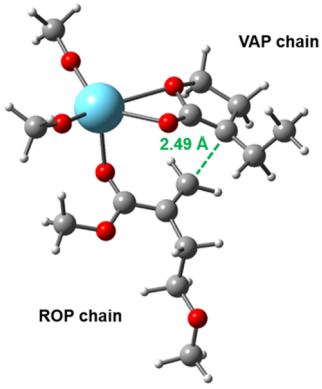

modulus (E'') of 119 MPa at −100 °C (glassy state), or E' = 160 MPa and E'' = 10.5 MPa at 25 °C (rubbery state). The T_g obtained from the peak maxima on the loss modulus curve was −21.9 °C, which is about 13 °C higher than that obtained from DSC analysis.

Postfunctionalization of the unsaturated polyester P-$(MBL)_{ROP}$ produced by **2** was examined with two different approaches. First, photocuring under UV (350 nm) photo-radical initiation with photoinitiator 2,2-dimethoxy-2-phenylacetophenone (DMPA) produced an insoluble cross-linked colorless thin film, $P(MBL)_{ROP}$-*hν*. The FT-IR spectrum (Figure S13) of the film showed similar features to those of $P(MBL)_{ROP}$, but with much weaker absorption bands corresponding to the >C═CH_2 moiety, suggesting that a considerable amount, but not all, of the vinylidene groups participated in the cross-linking (Scheme 4). No apparent T_g was observed for the cross-linked film, but its TGA and DTG

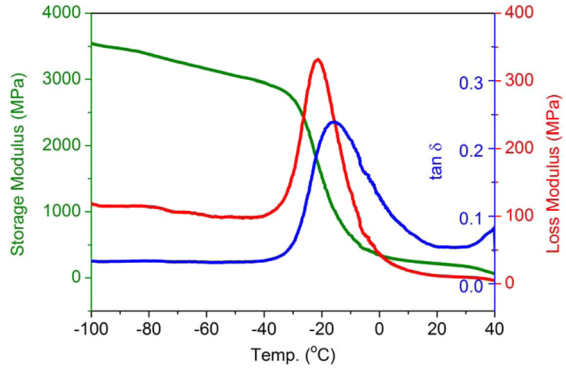

Figure 4. Thermal mechanical spectrum of $P(MBL)_{ROP}$ (M_n = 21.0 kg/mol, $Đ$ = 1.42) obtained by yttrium complex **2**: storage modulus E' (green curve), loss modulus E'' (red curve), and tan δ (E''/E') (blue curve).

Scheme 4. Postfunctionalization of $P(MBL)_{ROP}$ via Photocuring and the Thiol−Ene Click Reaction

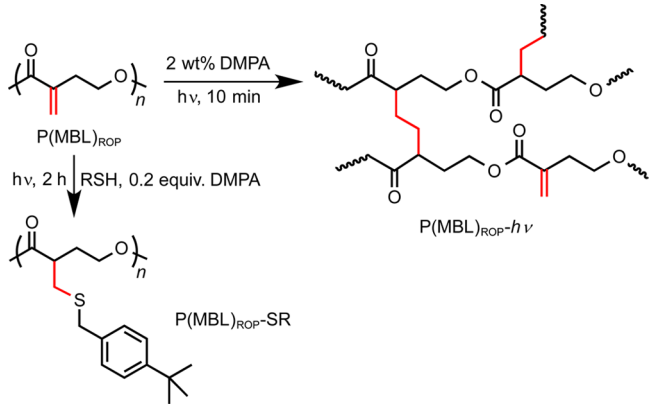

DOI: 10.1021/jacs.6b07974
J. Am. Chem. Soc. 2016, 138, 14326−14337

curves (Figure S14) are similar to that of $P(MBL)_{ROP}$ (Figure S10d), further confirming the hypothesis of $P(MBL)_{ROP}$ undergoing thermal cross-linking before decomposition during TGA analysis. On the other hand, photocuring of the low MW $P(MBL)_{ROP}$ prepared by **1**/BnOH (1:3) yielded $P(MBL)_{ROP}$-$h\nu$ with a TGA curve (Figure S15) being different than its precursor (Figure S10a), eliminating the initial MBL extrusion step. Worth noting here is that the cross-linked polymer $P(MBL)_{ROP}$-$h\nu$ produced by postphotocuring is different from the cross-linked polymer $P(MBL)_{CLP}$ as prepared by **1**/BnOH (1:1) at −60 °C, the latter of which contains mainly $P(MBL)_{VAP}$ chains with some ROP chains incorporated (vide supra). The second approach for postfunctionalization was readily realized by the thiol−ene click reaction,[30] which afforded completely thiolated polyester $P(MBL)_{ROP}$-SR (Scheme 4, Figures 5 and S16).

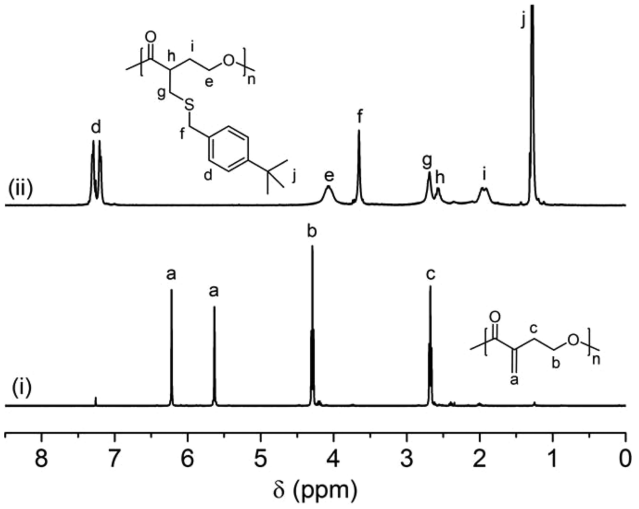

Figure 5. Overlay of ^{1}H NMR ($CDCl_3$) spectra of $P(MBL)_{ROP}$ and $P(MBL)_{ROP}$-SR to show complete conversion of >C═CH_2 groups present in $P(MBL)_{ROP}$ to >C═CH_2−SR in $P(MBL)_{ROP}$-SR.

Recycling and Degradation of $P(MBL)_{ROP}$. The possible recycling of $P(MBL)_{ROP}$ back to its building block monomer MBL was investigated by thermal and chemical recycling approaches. As anticipated, heating the bulk material at high temperatures resulted in formation of insoluble polymer products due to thermally induced cross-linking via the C═C double bonds present in the unsaturated polyester $P(MBL)_{ROP}$ (vide supra). Next, the depolymerization was performed at 25 °C in the presence of catalyst **1** to produce initially some MBL, which was subsequently polymerized by **1** into $P(MBL)_{VAP}$, plus some insoluble cross-linked material (Figure S17). This promising result prompted us to develop a strategy to inhibit the subsequent VAP once the monomer MBL is released from $P(MBL)_{ROP}$. Excitingly, heating a 0.2 M solution of $P(MBL)_{ROP}$ in DMSO-d_6 in the presence of **1** (1 mol %) and water (3.5 mM, added to inhibit polymerization) at 100 or 130 °C for 1 h, or 60 °C for 24 h, yielded cleanly the monomer MBL in quantitative yield (Figure 6, Table 2). Simple metal halides such as $LaCl_3$, which is incapable of reinitiating the VAP of MBL generated from depolymerization, can also be used as the catalyst to achieve complete chemical recycling of $P(MBL)_{ROP}$ back to MBL (Figure S18, Table S3).

The hydrolytic stability of $P(MBL)_{ROP}$ in aqueous media was evaluated by submerging the specimens in neutral (DI H_2O),

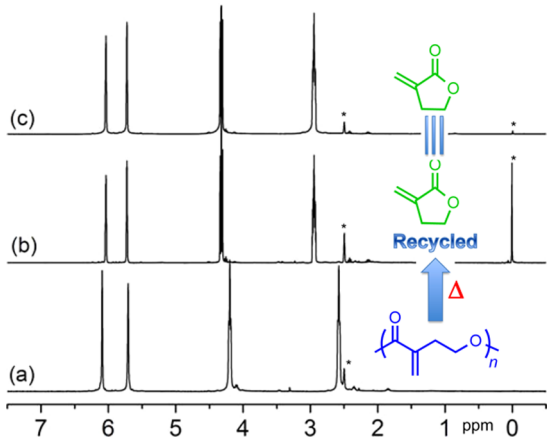

Figure 6. ^{1}H NMR spectra (DMSO-d_6): (a) $P(MBL)_{ROP}$ (M_n = 21.0 kg/mol); (b) the liquid product obtained after heating the "wet" DMSO solution with 3.5 mM water at 100 °C for 1 h; (c) MBL monomer for comparison. NMR solvent peaks marked as ∗.

acidic (1 M HCl), and basic (1 M NaOH) solutions under ambient conditions and monitoring the mass loss of the specimens over a period of 120 days. As can be seen from its degradation profiles (Figure 7, Table S4), $P(MBL)_{ROP}$ readily but gradually degraded in 1 M NaOH, with ∼97% of the mass loss after 120 days. In sharp contrast, $P(MBL)_{ROP}$ is rather stable in both DI H_2O and 1 M HCl, with only about 2−4% mass loss over the same time period. Interestingly, $P(MBL)_{VAP}$ can also be effectively degraded under basic conditions (1 M NaOH, ∼95% mass loss after 120 days, Table S4).

Computational Study of MBL Polymerization. The behavior of $La[N(SiMe_3)_2]_3$ and $La(OR)_3$ (R = ^{n}Bu, ^{i}Pr) as catalysts in the polymerization of MBL was investigated by density functional theory (DFT) calculations. For both types (amide and alkoxide) of catalysts, we investigated the general reactivity along the VAP and the ROP pathways to clarify in details the chain initiation and propagation mechanisms and to explain the effect of the nucleophilic groups attached to La on the polymerization chemoselectivity. To reduce the conformational flexibility of the experimentally used O^{n}Bu and O^{i}Pr groups in $La(OR)_3$, we used the OMe group, thus modeling the $La(OMe)_3$ catalyst. The scenarios considered and the relative free energies (kcal/mol) calculated in THF at T = −60 °C are shown in Scheme 5. The energy profiles of the favored ROP pathway by $La(OMe)_3$ and the favored VAP pathway by $La[N(SiMe_3)_2]_3$ are plotted in Figure 8.

Upon coordination of the monomer (M) to the metal (La) to form species **1-La-M** in Scheme 5, two possible chain activation pathways were studied. Along the VAP pathway, one OMe or $N(SiMe_3)_2$ group of the catalyst attacks the exocylic carbon atom of the vinylidene moiety in MBL, which leads to intermediate **2-VAP** with both oxygens of the monomer coordinated to the metal. Polymerization proceeds with coordination of another monomer to **2-VAP**, which leads to **3-VAP**. Nucleophilic attack of the C(α) atom of the activated MBL to the exocylic carbon atom of the vinylidene moiety in the newly coordinated MBL, via transition state **3−4-VAP**, leads to intermediate **4-VAP**, the process of which mimics the general chain growth step along the VAP pathway. In the ROP pathway, one OR or $N(SiMe_3)_2$ group of the catalyst attacks the carbonyl carbon atom of MBL, which leads to species **2-ROP** that evolves to species **3-ROP** through ring opening of

DOI: 10.1021/jacs.6b07974
J. Am. Chem. Soc. 2016, 138, 14326−14337

Table 2. Results of Depolymerization of $P(MBL)_{ROP}$ in the Presence of 1 in "Wet" DMSO-d_6[a]

				products		
$[P(MBL)_{ROP}]_0$ (M)	H_2O conc. in DMSO-d_6 (mM)	temperature (°C)	time (h)	MBL (%)	$P(MBL)_{ROP}$ (%)	$P(MBL)_{VAP}$ (%)
0.2	3.5	130	1	**100**	0	0
0.4	3.5	130	1	84.2	0	15.8
0.6	3.5	130	1	41.9	0	58.1
0.2	3.5	100	1	**100**	0	0
0.2	3.5	60	1	43.1	56.9	0
0.2	3.5	60	2	63.7	36.3	0
0.2	3.5	60	4	88.1	11.9	0
0.2	3.5	60	6	95.5	4.5	0
0.2	3.5	60	24	**100**	0	0
0.2	9.5	130	1	41.0	59.0	0
0.2	9.5	130	2	45.6	54.4	0
0.2	9.5	130	12	59.7	40.3	0
0.2	9.5	130	24	65.7	34.3	0
0.4	9.5	130	1	77.9	22.1	0
0.4	9.5	130	2	78.6	21.4	0
0.4	9.5	130	12	88.5	11.5	0
0.4	9.5	130	24	91.4	8.6	0

[a]Conditions: $P(MBL)_{ROP}$/**1** = 100:1, the amount of $P(MBL)_{ROP}$ (M_n = 21.0 kg/mol, produced by MBL/**2** = 100:1) and **1** varied according to initial $P(MBL)_{ROP}$ concentration and $[P(MBL)_{ROP}]/[\mathbf{1}]$ molar ratio.

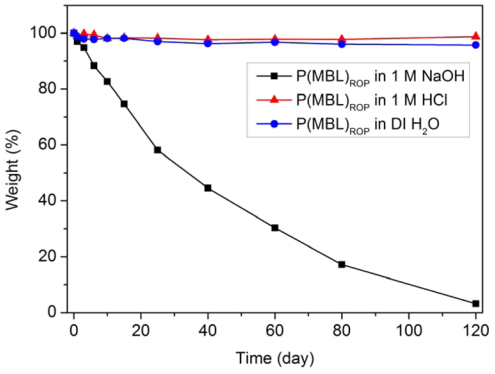

Figure 7. Degradation profiles of $P(MBL)_{ROP}$ in aqueous media.

the monomer via transition state **2−3-ROP**. The whole coordination−insertion event is repeated in each propagation step with the monomer inserting into the La−O bond via transition state **4−5-ROP** in Scheme 5.

According to calculations, the propensity of the two catalysts to promote activation along the ROP or the VAP pathway is opposite. By focusing on the selectivity determining **1−2-VAP** and **1−2-ROP** transition states, **1−2-ROP** is favored by almost 4 kcal/mol relative to **1−2-VAP** with $La(OMe)_3$, whereas **1−2-VAP** is favored by 7.4 kcal/mol relative to **1−2-ROP** with $La[N(SiMe_3)_2]_3$, which indicates that $La(OMe)_3$ and $La[N(SiMe_3)_2]_3$ promote the polymerization along the ROP and VAP pathways, respectively. The steric hindrance of the $SiMe_3$ groups in $La[N(SiMe_3)_2]_3$ accounts for the strong selectivity favoring attack at the more open vinylidene moiety since it minimizes steric repulsion with the other $SiMe_3$ substituents and with the monomer. In terms of absolute energy barriers, they are clearly lower with $La(OMe)_3$, consistent with the higher polarity of the La−O bond relative to the La−N bond (the atomic charge on the La atom is +1.79e in $La[OMe]_3$ and +1.69e in $La[N(SiMe_3)_2]_3$).

By focusing on the favored ROP pathway with $La(OMe)_3$, the propagation barrier of 12.5 kcal/mol for ring-opening along the generic chain growth step, corresponding to the **4-ROP** to **5-ROP** step, is consistent with the initiation barrier of 12.6

Scheme 5. Free Energies (kcal/mol in THF at −60 °C) of ROP and VAP Processes Catalyzed by $La[N(SiMe_3)_2]_3$ and $La(OMe)_3$ Catalysts

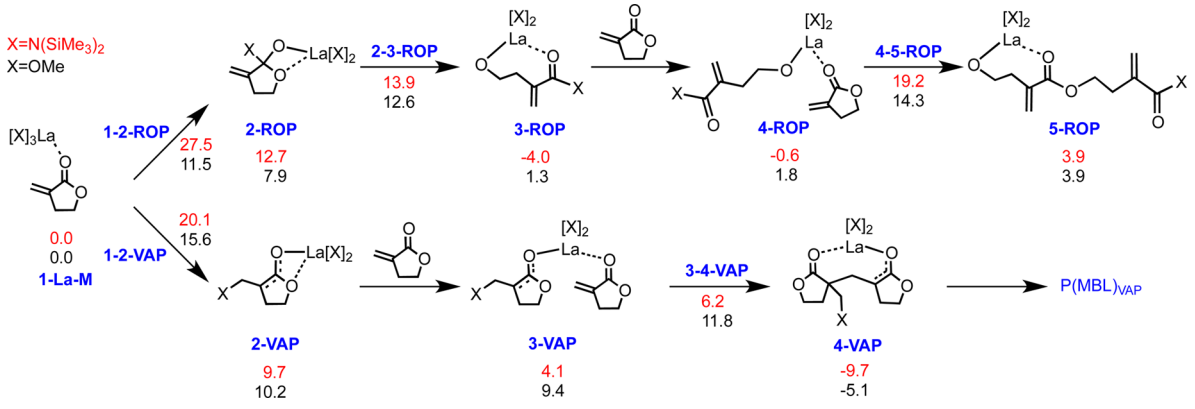

DOI: 10.1021/jacs.6b07974
J. Am. Chem. Soc. 2016, 138, 14326−14337

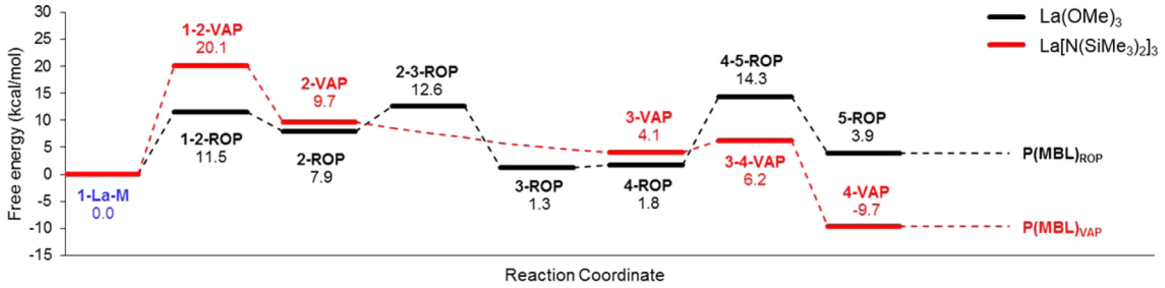

Figure 8. Free energy profiles (kcal/mol in THF at −60 °C) of the ROP of MBL catalyzed by $La(OMe)_3$ (black lines) and the VAP of MBL catalyzed by $La[N(SiMe_3)_2]_3$ (red lines).

kcal/mol for the **1-La-M** to **2-ROP** to **3-ROP** step. This is an expected result since in both cases it corresponds to insertion of MBL into a La−alkoxide bond. Differently, for the system bearing the $N(SiMe_3)_2$ groups, the propagation barrier from **4-ROP** to **5-ROP** is 7.7 kcal/mol lower than the barrier for the **1-La-M** to **2-ROP** initiation step (i.e., 19.8 vs 27.5 kcal/mol) since initiation involves MBL addition to a La−amide bond, while propagation involves MBL addition to a more polarized La−alkoxide bond. Moreover, the general transition state for MBL addition to a chain−$La[N(SiMe_3)_2]_2$ bond is higher than for addition to a chain−$La[OMe]_2$ bond, as consequence of the stronger partial positive charge on the La atom (+1.77e and +1.62e for the system bearing the OMe and the $N(SiMe_3)_2$ ligand, respectively).

The challenging thermodynamic scenario for the ROP shown in Scheme 5 and Figure 8 is consistent with low temperature (i.e., −60 °C) and high monomer concentration (i.e., 5.0 M) conditions required experimentally to favor the ROP. This behavior is directly related to the reduced reactivity of five-membered lactones toward ring opening due to the relative low strain energy (i.e., high thermodynamic stability) of the ring. To have an estimate of the energy cost related to the generic monomer addition through the ROP pathway, we calculated the free energy of the reaction shown in Scheme 6. According to the calculations, the forward reaction depicted in Scheme 6 is unfavored by 4.9 kcal/mol in free energy at −60 °C, consistently with the low ring strain of MBL, which makes the generic MBL addition step close to thermoneutral in terms of enthalpy but clearly disfavored in terms of entropy. As expected, the same analysis performed at lower temperatures reduces the unfavorable translational and rotational entropic terms, which make the forward reaction unfavored by only 1.8 kcal/mol at −126 °C and slightly favored by 0.7 kcal/mol, at −150 °C. These results are consistent with the observed extremely low ceiling temperature of the ROP of MBL at $[MBL]_0$ = 1.0 M (vide supra). Moving to the VAP pathway, the energy barrier calculated for the general chain growth step from **3-VAP** to **4-VAP**, roughly 2 kcal/mol, is much lower relative to the initiation barrier for both catalysts.

Scheme 6. Reaction Used To Model the Thermodynamics of the Generic MBL Polymerization Reaction

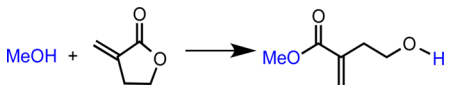

Overall, these results indicate a clear preference for initiation along the ROP pathway when −OR groups are bound to the metal, and an easier activation along the VAP pathway when bulky $-NR_2$ groups are bound to the metal. While the preferential activation along the VAP pathway with $La[N(SiMe_3)_2]_3$ is a clear consequence of the steric bulkiness of the $N(SiMe_3)_2$ groups, the preferential activation along the ROP activation with $La(OMe)_3$ deserves a more detailed analysis. To this end, we explored the capability of different nucleophiles to modify the stability of the adducts from addition to the methylidene or to the cabonylic C atoms. The data reported in Table 3 indicate that in the absence of a group activating the C═O moiety, vinyl addition is favored over addition to the carbonyl group. This preference is related to delocalization of the negative charge on the four atoms of the MBL moiety in case of addition to the vinyl group, while the negative charge is substantially localized on the exocyclic O atom in case of addition at the carbonyl group. However, coordination of MBL to the $La(OMe)_3$ moiety renders OMe^- attack to the carbonyl group thermodynamically favored by 3.2 kcal/mol (Table 3). Interestingly, the activating capability of a simple H^+ is comparable to that of the $La(OMe)_3$ moiety.

Next, we examined the behavior of yttrium alkyl species Y-**2** and Y-**3** (Chart 1) as catalysts in the ROP of MBL. The scenario considered and the relative free energies calculated in THF at −60 °C are shown in Scheme 7. According to our calculations, replacing the coordinated THF by a MBL molecule is slightly endergonic. The **1**−**2-ROP** transition state is placed 18.5 kcal/mol above the starting precatalyst. Remarkably, the initiation event leading to **2-ROP** is thermodynamically favored, by roughly 17 kcal/mol, with Y-**2**, while it is endergonic by roughly 8 kcal/mol with $La(OMe)_3$ (Scheme 5). To test if this is a consequence of the steric or

Table 3. Stability of the Adducts Deriving from Nucleophilic Attack to the Methylidene (CH_2═C) or to the Carbonyl Group (C═O) of MBL[a]

reaction	E (CH_2═C)	E (C═O)	ΔE (C═O−CH_2═C)
MeO^- + MBL → $(MeO\text{-}MBL)^-$	−23.6	−15.7	7.9
$La(OMe)_3$ + MBL → MeO-MBL-$La(OMe)_2$	7.0	3.8	−3.2
MeO^- + MBL-H^+ → MeO-MBL-H	−74.3	−80.1	−5.8

[a]Energies in kcal/mol.

DOI: 10.1021/jacs.6b07974
J. Am. Chem. Soc. 2016, 138, 14326−14337

Scheme 7. Free Energies (kcal/mol in THF at T = −60 °C) Associated with the ROP of MBL Catalyzed by Y-2

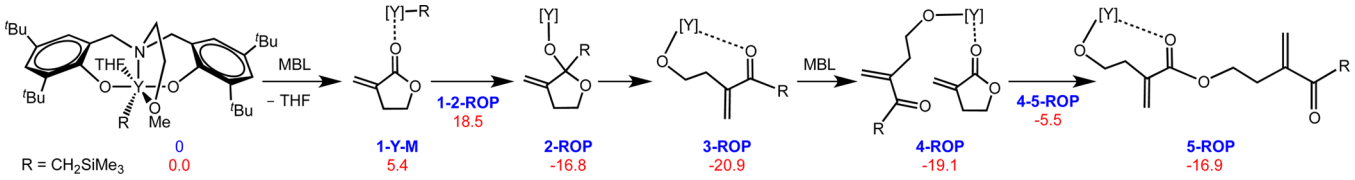

Scheme 8. Free Energies (kcal/mol in THF at T = −60 °C) of Different Isomers of the Intermediates along the ROP Pathway Catalyzed by Y-2

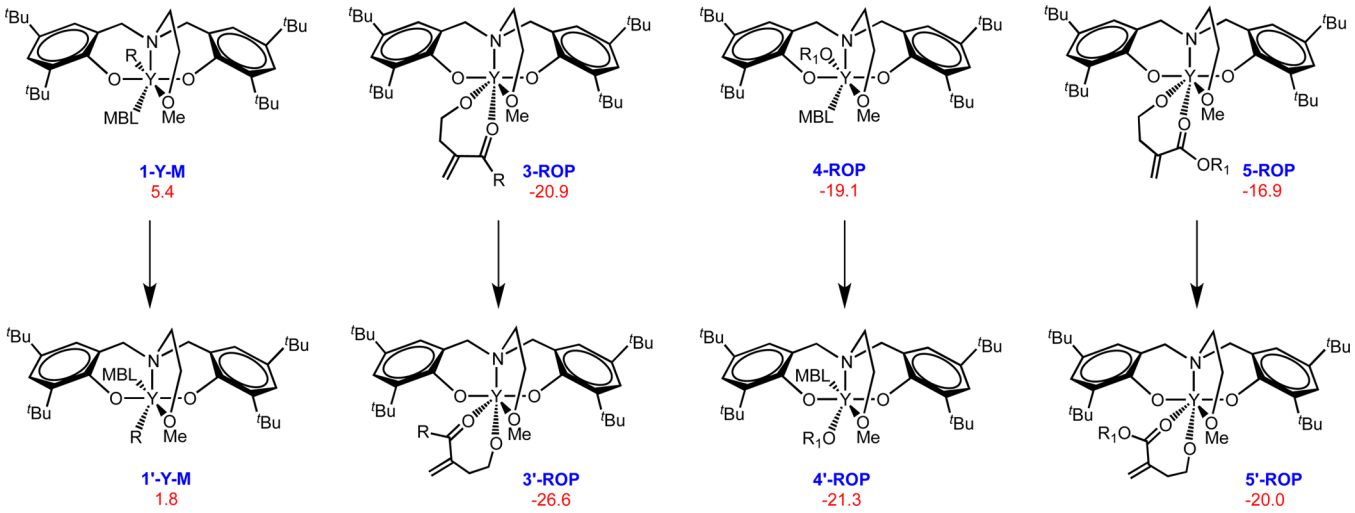

electronic situation at Y-**2**, we calculated the thermodynamics of the **1-Y-M** to **2-ROP** step with a modified model of Y-**2** where the migrating $-CH_2SiMe_3$ group is replaced by a −OMe group. According to calculations, migration of the −OMe group is thermoneutral, which suggests that the main reason is electronic, specifically, in the balance between the strength of the La−C bond in the starting Y-**2** versus the La−O bond in **2-ROP**.

As additional tests, we probed initiation along the possible VAP pathway. Consistent with the experimental results, our calculation showed that transition state **1−2-VAP** is 1.2 kcal/mol above transition state **1−2-ROP**. Furthermore, we also calculated initiation with Y-**3** and found transition state **1−2-ROP** with Y-**3** is 0.4 kcal/mol above the same transition state with Y-**2**, in qualitative agreement with the reduced ROP activity of Y-**3**.

As a final remark, we note that the preferred **1−2-ROP** transition state depicted in Scheme 7 shows the MBL *trans* to the OMe group of the ligand. For this reason, the entire pathway of Scheme 7 is built assuming that coordination of MBL to Y occurs *trans* to the OMe group. The energetic balance between different intermediates along the reaction pathway is shown in Scheme 8. Isomerization between **1-Y-M** and **1′-Y-M** as well as between **4-ROP** and **4′-ROP** can be assumed to occur via dissociation of MBL, while isomerization between **3-ROP** and **3′-ROP** as well as between **5-ROP** and **5′-ROP** can be assumed to occur via dissociation of the coordinated C═O group of the penultimate inserted MBL.

■ CONCLUSIONS

Through this study, we have uncovered the thermodynamic (T_c = −52 °C, $[MBL]_0$ = 5.0 M), catalytic (La and Y catalysts), and processing (THF for polymer precipitation) conditions that enabled the first successful ROP of the biorenewable MBL, achieving exclusively unsaturated polyester $P(MBL)_{ROP}$ via the proposed coordination−insertion mechanism. As MBL is a bifunctional monomer containing both the highly reactive exocyclic C═C bond and the highly stable nonstrained γ-BL ring, achieving the ROP of MBL by reversing the conventional VAP chemoselectivity through this work is particularly noteworthy. This work also discovered the third reaction pathway for the polymerization of MBL: crossover propagation, enabled by coexisting VAP and ROP processes that can also crossover, which leads to cross-linked polymer product $P(MBL)_{CLP}$ having predominately VAP chains.

Homoleptic lanthanum amide **1** is a versatile catalyst that produces three types of polymers according to the catalyst/initiator ratio: $P(MBL)_{VAP}$, $P(MBL)_{CLP}$, and $P(MBL)_{ROP}$ can be readily produced with a **1**/ROH ratio of 1:0, 1:1, and 1:3, respectively. This remarkable product selectivity, as controlled by the **1**/ROH ratio, is originated from the unique chemoselectivity uncovered by this study: the La−NR_2 group leads to the VAP process, while the La−OR group favors the ROP. On the other hand, heteroleptic, discrete single-site yttrium alkyl catalyst/initiator **2** undergoes exclusive ROP and also delivers the best overall performance, which produces $P(MBL)_{ROP}$ with M_n up to 21.0 kg/mol.

The thermal analysis showed that $P(MBL)_{ROP}$ exhibits a T_g in the range of −40.2 to −34.9 °C, depending on the polymer MW, and a two-step decomposition profile with an initial T_d of 293 °C (for a sample with M_n = 18.3 kg/mol) due to thermal cross-linking before decomposition. $P(MBL)_{ROP}$ can be readily postfunctionalized via photocuring and the thiol−ene click reaction into cross-linked or thiolated materials. The hydrolytic stability study revealed that $P(MBL)_{ROP}$ is readily degradable under basic conditions. Most remarkably, $P(MBL)_{ROP}$ can be

DOI: 10.1021/jacs.6b07974
J. Am. Chem. Soc. 2016, 138, 14326−14337

fully recycled back to its monomer MBL after its solution is heated at ≥100 °C for 1 h in the presence of a simple catalyst, which thus establishes its complete chemical recyclability.

DFT calculations satisfactorily explained the low temperature condition that must be met to achieve the ROP of the MBL. Theoretical investigation of the experimentally observed three different polymerization processes (VAP, ROP, and CLP) involved in the polymerization of MBL revealed that the sterics are responsible for the preference of La−NR_2 group for the VAP pathway, while the electronics are the reason for the favored ROP pathway by La−OR group.

■ ASSOCIATED CONTENT

Supporting Information

The Supporting Information is available free of charge on the ACS Publications website at DOI: 10.1021/jacs.6b07974.

Full experimental and computational details; additional figures and tables (PDF)

■ AUTHOR INFORMATION

Corresponding Authors

*E-mail: luigi.cavallo@kaust.edu.sa.

*E-mail: eugene.chen@colostate.edu.

Notes

The authors declare the following competing financial interest(s): A provisional patent application was filed on April 10, 2015 and a subsequent PCT International patent application was filed on April 11, 2016.

■ ACKNOWLEDGMENTS

This work was supported by the US National Science Foundation (NSF-1300267) for the study carried out at Colorado State University and by the funding from King Abdullah University of Science and Technology (KAUST) for the study performed at KAUST.

■ REFERENCES

(1) Selected reviews: (a) Gandini, A.; Lacerda, T. M.; Carvalho, A. J. F.; Trovatti, E. *Chem. Rev.* **2016**, *116*, 1637−1669. (b) Galbis, J. A.; García-Martín, G.; de Paz, V.; Galbis, E. *Chem. Rev.* **2016**, *116*, 1600−1636. (c) Delidovich, I.; Hausoul, P. J. C.; Deng, L.; Pfützenreuter, R.; Rose, M.; Palkovits, R. *Chem. Rev.* **2016**, *116*, 1540−1599. (d) Gandini, A.; Lacerda, T. M. *Prog. Polym. Sci.* **2015**, *48*, 1−39. (e) Vilela, C.; Sousa, A. F.; Fonseca, A. C.; Serra, A.; Coelho, J. F. J.; Freire, C. S. R.; Silvestre, A. J. D. *Polym. Chem.* **2014**, *5*, 3119−3141. (f) Tschan, M. J.-L.; Brulé, E.; Haquette, P.; Thomas, C. M. *Polym. Chem.* **2012**, *3*, 836−851. (g) Coates, G. W.; Hillmyer, M. A. *Macromolecules* **2009**, *42*, 7987−7989. (h) Gandini, A. *Macromolecules* **2008**, *41*, 9491−9504. (i) Williams, C. K.; Hillmyer, M. A. *Polym. Rev.* **2008**, *48*, 1−10. (j) Meier, M. A. R.; Metzger, J. O.; Schubert, U. S. *Chem. Soc. Rev.* **2007**, *36*, 1788−1802.

(2) Hong, M.; Chen, E. Y.-X. *Nat. Chem.* **2015**, *8*, 42−49.

(3) Diesendruck, C. E.; Peterson, G. I.; Kulik, H. J.; Kaitz, J. A.; Mar, B. D.; May, P. A.; White, S. R.; Martínez, T. J.; Boydston, A. J.; Moore, J. S. *Nat. Chem.* **2014**, *6*, 623−628.

(4) (a) Schneiderman, D. K.; Vanderlaan, M. E.; Mannion, A. M.; Panthani, T. R.; Batiste, D. C.; Wang, J. Z.; Bates, F. S.; Macosko, C. W.; Hillmyer, M. A. *ACS Macro Lett.* **2016**, *5*, 515−518. (b) MacDonald, J. P.; Shaver, M. P. *Polym. Chem.* **2016**, *7*, 553−559.

(5) (a) Kopinke, F.-D.; Remmler, M.; Mackenzie, K.; Moder, M.; Wachsen, O. *Polym. Degrad. Stab.* **1996**, *53*, 329−342. (b) McNeill, I. C.; Leiper, H. A. *Polym. Degrad. Stab.* **1985**, *11*, 309−326.

(6) Hong, M.; Chen, E. Y.-X. *Angew. Chem., Int. Ed.* **2016**, *55*, 4188−4193.

(7) Selected reviews: (a) Kitson, R. R. A.; Millemaggi, A.; Taylor, R. J. K. *Angew. Chem., Int. Ed.* **2009**, *48*, 9426−9451. (b) Hoffmann, H. M. R.; Rabe, J. *Angew. Chem., Int. Ed. Engl.* **1985**, *24*, 94−110.

(8) Selected reviews: (a) Gowda, R. R.; Chen, E. Y.-X. *Encyclopedia of Polymer Science and Technology*, 4th ed.; Mark, H. F., Ed.; Wiley: Hoboken, NJ, 2014; Vol. *8*, pp 235−271. DOI: 10.1002/0471440264.pst606. (b) Agarwal, S.; Jin, Q.; Maji, A. *ACS Symp. Ser.* **2012**, *1105*, 197−212. (c) Mullin, R. *Chem. Eng. News* **2004**, *82* (45), 29−37.

(9) (a) Manzer, L. E. *ACS Symp. Ser.* **2006**, *921*, 40−51. (b) Manzer, L. E. *Appl. Catal., A* **2004**, *272*, 249−256.

(10) Gowda, R. R.; Chen, E. Y.-X. *Org. Chem. Front.* **2014**, *1*, 230−234.

(11) (a) Vobecka, Z.; Wei, C.; Tauer, K.; Esposito, D. *Polymer* **2015**, *74*, 262−271. (b) Lee, C.; Song, K. *Asian J. Chem.* **2014**, *26*, 8057−8061. (c) Shin, J.; Lee, Y.; Tolman, W. B.; Hillmyer, M. A. *Biomacromolecules* **2012**, *13*, 3833−3840. (d) Higaki, Y.; Okazaki, R.; Takahara, A. *ACS Macro Lett.* **2012**, *1*, 1124−1127. (e) Cockburn, R. A.; Siegmann, R.; Payne, K. A.; Beuermann, S.; McKenna, T. F. L.; Hutchinson, R. A. *Biomacromolecules* **2011**, *12*, 2319−2326. (f) Juhari, A.; Mosnáček, J.; Yoon, J. A.; Nese, A.; Koynov, K.; Kowalewski, T.; Matyjaszewski, K. *Polymer* **2010**, *51*, 4806−4813. (g) Mosnáček, J.; Yoon, J. A.; Juhari, A.; Koynov, K.; Matyjaszewski, K. *Polymer* **2009**, *50*, 2087−2094. (h) Qi, G.; Nolan, M.; Schork, F. J.; Jones, C. W. *J. Polym. Sci., Part A: Polym. Chem.* **2008**, *46*, 5929−5944. (i) Mosnáček, J.; Matyjaszewski, K. *Macromolecules* **2008**, *41*, 5509−5511. (j) Pittman, C. U., Jr.; Lee, H. *J. Polym. Sci., Part A: Polym. Chem.* **2003**, *41*, 1759−1777. (k) Stansbury, J. W.; Antonucci, J. M. *Dent. Mater.* **1992**, *8*, 270−273. (l) Ueda, M.; Takahashi, M.; Imai, Y.; Pittman, C. U. *J. Polym. Sci., Polym. Chem. Ed.* **1982**, *20*, 2819−2828. (m) Akkapeddi, M. K. *Polymer* **1979**, *20*, 1215−1216. (n) Akkapeddi, M. K. *Macromolecules* **1979**, *12*, 546−551.

(12) (a) Hu, Y.; Gustafson, L. O.; Zhu, H.; Chen, E. Y.-X. *J. Polym. Sci., Part A: Polym. Chem.* **2011**, *49*, 2008−2017. (b) Suenaga, J.; Sutherlin, D. M.; Stille, J. K. *Macromolecules* **1984**, *17*, 2913−2916.

(13) (a) Chen, J.; Chen, E. Y.-X. *Molecules* **2015**, *20*, 9575−9590. (b) Xu, T.; Chen, E. Y.-X. *J. Am. Chem. Soc.* **2014**, *136*, 1774−1777. (c) Zhang, Y.; Miyake, G. M.; John, M. G.; Falivene, L.; Caporaso, L.; Cavallo, L.; Chen, E. Y.-X. *Dalton Trans.* **2012**, *41*, 9119−9134. (d) Zhang, Y.; Miyake, G. M.; Chen, E. Y.-X. *Angew. Chem., Int. Ed.* **2010**, *49*, 10158−10162.

(14) (a) Zhang, Y.; Gustafson, L. O.; Chen, E. Y.-X. *J. Am. Chem. Soc.* **2011**, *133*, 13674−13684. (b) Miyake, G. M.; Zhang, Y.; Chen, E. Y.-X. *Macromolecules* **2010**, *43*, 4902−4908. (c) Sogah, D. Y.; Hertler, W. R.; Webster, O. W.; Cohen, G. M. *Macromolecules* **1987**, *20*, 1473−1488.

(15) (a) Gowda, R. R.; Chen, E. Y.-X. *ACS Macro Lett.* **2016**, *5*, 772−776. (b) Schmitt, M.; Falivene, L.; Caporaso, L.; Cavallo, L.; Chen, E. Y.-X. *Polym. Chem.* **2014**, *5*, 3261−3270. (c) Zhang, Y.; Schmitt, M.; Falivene, L.; Caporaso, L.; Cavallo, L.; Chen, E. Y.-X. *J. Am. Chem. Soc.* **2013**, *135*, 17925−17942. (d) Zhang, Y.; Chen, E. Y.-X. *Angew. Chem., Int. Ed.* **2012**, *51*, 2465−2469.

(16) (a) Gowda, R. R.; Caporaso, L.; Cavallo, L.; Chen, E. Y.-X. *Organometallics* **2014**, *33*, 4118−4130. (b) Hu, Y.; Wang, X.; Chen, Y.; Caporaso, L.; Cavallo, L.; Chen, E. Y.-X. *Organometallics* **2013**, *32*, 1459−1465. (c) Gowda, R. R.; Chen, E. Y.-X. *Dalton Trans.* **2013**, *42*, 9263−9273. (d) Chen, X.; Caporaso, L.; Cavallo, L.; Chen, E. Y.-X. *J. Am. Chem. Soc.* **2012**, *134*, 7278−7281. (e) Hu, Y.; Xu, X.; Zhang, Y.; Chen, Y.; Chen, E. Y.-X. *Macromolecules* **2010**, *43*, 9328−9336.

(17) (a) Johnson, K. G.; Yang, L. S. Preparation, Properties, and Applications of Unsaturated Polyester. *Modern Polyesters: Chemistry and Technology of Polyesters and Copolyesters*; Scheirs, J., Long, T. E., Eds.; Wiley: Chichester, UK, 2003; pp 699−713. (b) Boenig, H. V. *Unsaturated Polyesters: Structure and Properties*; Elsevier, 1964.

(18) Selected reviews: (a) Carpentier, J.-F. *Organometallics* **2015**, *34*, 4175−4189. (b) Hillmyer, M. A.; Tolman, W. B. *Acc. Chem. Res.* **2014**, *47*, 2390−2396. (c) Sauer, A.; Kapelski, A.; Fliedel, C.; Dagorne, S.; Kol, M.; Okuda, J. *Dalton Trans.* **2013**, *42*, 9007−9023. (d) Lecomte, P.; Jérôme, C. *Adv. Polym. Sci.* **2011**, *245*, 173−217. (e) Kiesewetter,

M. K.; Shin, E. J.; Hedrick, J. L.; Waymouth, R. M. *Macromolecules* **2010**, *43*, 2093−2107. (f) Carpentier, J.-F. *Macromol. Rapid Commun.* **2010**, *31*, 1696−1705. (g) Jérôme, C.; Lecomte, P. *Adv. Drug Delivery Rev.* **2008**, *60*, 1056−1076. (h) Kamber, N. E.; Jeong, W.; Waymouth, R. M.; Pratt, R. C.; Lohmeijer, B. G. G.; Hedrick, J. L. *Chem. Rev.* **2007**, *107*, 5813−5840. (i) Albertsson, A.-C.; Varma, I. K. *Biomacromolecules* **2003**, *4*, 1466−1486. (j) Albertsson, A.-C.; Varma, I. K. *Adv. Polym. Sci.* **2002**, *157*, 1−40. (k) O'Keefe, B. J.; Hillmyer, M. A.; Tolman, W. B. *Dalton Trans.* **2001**, 2215−2224. (l) Mecerreyes, D.; Jerome, R.; Dubois, P. *Adv. Polym. Sci.* **1999**, *147*, 1−59. (m) Kuran, W. *Prog. Polym. Sci.* **1998**, *23*, 919−992.

(19) Uyama, H.; Kobayashi, S.; Morita, M.; Habaue, S.; Okamoto, Y. *Macromolecules* **2001**, *34*, 6554−6556.

(20) (a) Allcock, H. R.; Lampe, F. W.; Mark, J. E. *Contemporary Polymer Chemistry*, 3rd ed.; Pearson Education Inc.: Upper Saddle River, NJ, 2003; p 155. (b) Odian, G. *Principles of Polymerization*, 3rd ed.; Wiley-Interscience: New York, 1991; p 570. (c) Sawada, H. *Thermodynamics of Polymerization*; Marcel Dekker, Inc.: New York, 1976; p 150.

(21) Houk, K. H.; Jabbari, A.; Hall, H. K., Jr.; Alemán, C. *J. Org. Chem.* **2008**, *73*, 2674−2678.

(22) (a) Duda, A.; Penczek, S.; Dubois, P.; Mecerreyes, D.; Jérôme, R. *Macromol. Chem. Phys.* **1996**, *197*, 1273−1283. (b) Duda, A.; Biela, T.; Libiszowski, J.; Penczek, S.; Dubois, P.; Mecerreyes, D.; Jérôme, R. *Polym. Degrad. Stab.* **1998**, *59*, 215−222.

(23) (a) Olsén, P.; Odelius, K.; Albertsson, A.-C. *Biomacromolecules* **2016**, *17*, 699−709. (b) Duda, A.; Kowalski, A. *Handbook of Ring-Opening Polymerization*; Dubois, P., Coulembier, O., Raquez, J.-M., Eds.; Wiley-VCH: Weinheim, 2009; pp 1−51. (c) Alemán, C.; Betran, O.; Casanovas, J.; Houk, K. H.; Hall, H. K., Jr. *J. Org. Chem.* **2009**, *74*, 6237−6244. (d) Saiyasombat, W.; Molloy, R.; Nicholson, T. M.; Johnson, A. F.; Ward, I. M.; Poshyachinda, S. *Polymer* **1998**, *39*, 5581−5585.

(24) Zhou, J.; Schmidt, A. M.; Ritter, H. *Macromolecules* **2010**, *43*, 939−942.

(25) Hong, M.; Chen, E. Y.-X. *Macromolecules* **2014**, *47*, 3614−3624.

(26) Amgoune, A.; Thomas, C. M.; Roisnel, T.; Carpentier, J. F. *Chem. - Eur. J.* **2006**, *12*, 169−179.

(27) Liu, X.; Shang, X.; Tang, T.; Hu, N.; Pei, F.; Cui, D.; Chen, X.; Jing, X. *Organometallics* **2007**, *26*, 2747−2757.

(28) Ma, H.; Okuda, J. *Macromolecules* **2005**, *38*, 2665−2673.

(29) Chen, E. Y.-X. *Chem. Rev.* **2009**, *109*, 5157−5214.

(30) Selected reviews: (a) Barner-Kowollik, C.; Du Prez, F. E.; Espeel, P.; Hawker, C. J.; Junkers, T.; Schlaad, H.; Van Camp, W. *Angew. Chem., Int. Ed.* **2011**, *50*, 60−62. (b) Hoyle, C. E.; Bowman, C. N. *Angew. Chem., Int. Ed.* **2010**, *49*, 1540−1573. (c) Iha, R. K.; Wooley, K. L.; Nyström, A. M.; Burke, D. J.; Kade, M. J.; Hawker, C. J. *Chem. Rev.* **2009**, *109*, 5620−5686. (d) Binder, W. H.; Sachsenhofer, R. *Macromol. Rapid Commun.* **2008**, *29*, 952−981. (e) Binder, W. H.; Sachsenhofer, R. *Macromol. Rapid Commun.* **2007**, *28*, 15−54.

DOI: 10.1021/jacs.6b07974
J. Am. Chem. Soc. 2016, 138, 14326−14337